

Multi-Arc Filtering During the Navigation Campaign of the OSIRIS-REx Mission

Andrew S. French^{1,3}, Jason M. Leonard¹, Jeroen L. Geeraert¹, Brian R. Page¹, Peter G. Antreasian¹, Michael C. Moreau², Jay W. McMahon³, Daniel J. Scheeres³, and the OSIRIS-REx Team

¹KinetX, Inc., Space Navigation and Flight Dynamics Practice, 21 W. Easy St., Ste 108, Simi Valley, CA 93065, USA

²NASA/GSFC Navigation and Mission Design Branch, 8800 Greenbelt Rd, Greenbelt, MD 20771, USA

³Smead Aerospace Engineering Sciences, University of Colorado, 2598 Colorado Ave, Boulder, CO 80302

The Navigation Campaign of the OSIRIS-REx mission consisted of three phases: Approach, Preliminary Survey and Orbital-A. These phases were designed to optimize the initial characterization of Bennu’s mass, shape and spin-state to support a safe orbit insertion and a quick transition to landmark-based optical navigation tracking. The standard orbit determination filtering techniques used to navigate the spacecraft were unable to fit data from these three phases simultaneously due to numerical issues associated with the nonlinear dynamics and the long arc length. Consequently, a multi-arc filtering algorithm was implemented in order to combine the information from each of these arcs. Multi-arc solutions for Bennu’s spin state and gravity field are presented here.

1. Extended Abstract

1.1. Introduction

The Origins Spectral Interpretation Resource Identification Security Regolith Explorer (OSIRIS-REx) mission is America’s first asteroid sampler-return mission. Launched in September 2016, the OSIRIS-REx spacecraft obtained the first image of its target, asteroid 101955 Bennu (1999 RQ36), on August 17th, 2018.¹ This marked the start of the Approach phase, the first in three successive phases comprising OSIRIS-REx’s Navigation Campaign. These phases include Approach, Preliminary Survey and Orbital-A.² The Approach phase allowed for precise estimation of Bennu’s ephemeris and preliminary shape model construction. In addition, several high-resolution rotation movies were taken which allowed the orbit determination (OD) team to produce an initial spin state estimate. Preliminary Survey consisted of five hyperbolic flybys each with a close approach radius of about 7 km. Each flyby added additional information about Bennu’s mass and shape, resulting in a GM estimate good to 1% that fed into the nominal Orbital-A design.^{3,4} Orbital-A placed the spacecraft in a 2.1x1.5 km frozen orbit, which remained stable throughout its two month duration. During this time the optical navigation (OpNav), OD and Altimetry Working Group (ALTWG) teams collaborated to produce precise estimates of Bennu’s spin state and center-of-figure to center-of-mass offset, after which time the OD team transitioned from using center-finding based OpNavs to landmark-based OpNavs.

Due to the highly nonlinear nature of the Preliminary Survey phase the standard filtering techniques used to navigation the spacecraft were not able to fit all of the Navigation Campaign data simultaneously. Multi-arc filtering is a process of combining solutions from several independent arcs to produce a single estimate of the parameters common to each arc. The need for this technique was first employed by Kaula on Earth observing satellites and has subsequently been used for the gravity field reconstructions of asteroid Eros, Saturn and its moons, and many other bodies.⁵⁻⁸

This paper will step through how multi-arc filtering was used to validate orbit determination performance during the Navigation Campaign. First, focus will be given to the estimation of Bennu’s GM during the Preliminary Survey phase prior to orbit insertion. The result will be compared to the estimate produced by the entirety of Orbital-A. Next, information about the low degree and order (3x3) gravity field harmonics will be characterized using all available data from the Approach, Preliminary Survey and Orbital-A phases. Finally, landmark optical navigation data from the high-resolution rotation movies taken during Approach will be combined with the two months of Orbital-A data to produce a spin state estimate that spans the full duration of the Navigation Campaign.

Results for the GM estimate prior to orbit insertion can be seen in Figure 1 and Table 1.

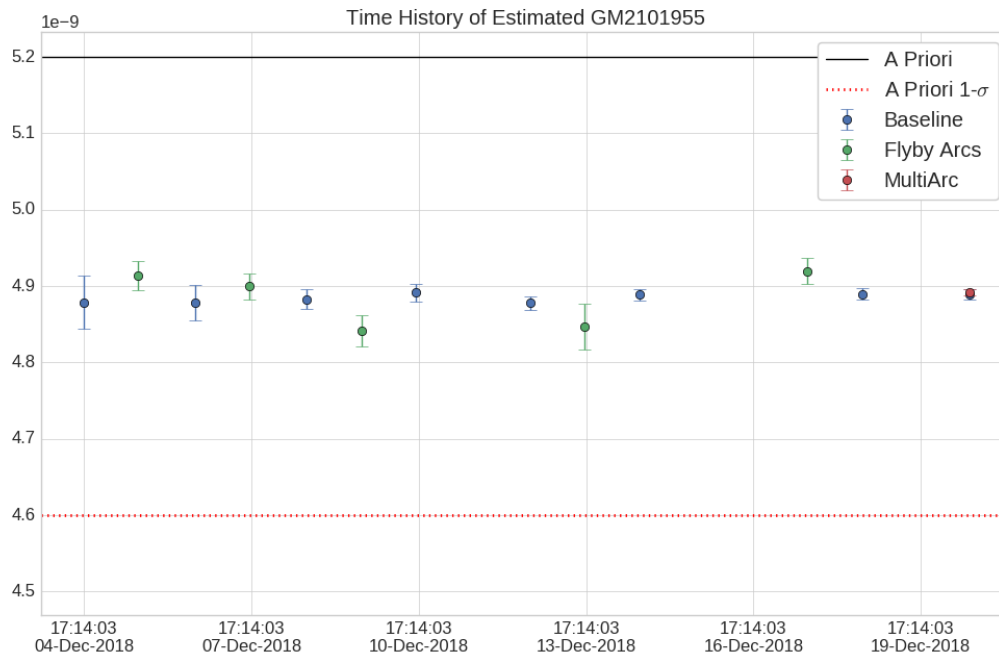


Figure 1: Estimated GM during preliminary survey. The black and red lines denote the *a priori* estimate and 1σ respectively.⁹ Long arc filter solutions with their estimated 1σ s are in blue and plotted at their respective data cutoffs. Flyby arcs are shown in green and the multi-arc solution, which combines information from each of the individual flyby arcs, is shown in red.

Table 1: Summary of GM estimates. Each flyby arc spans approximately 48 hours.

Arc	Estimated Value	Estimated Sigma
North Pole Flyby #1	4.914	0.019
North Pole Flyby #2	4.900	0.017
North Pole Flyby #3	4.842	0.020
Equatorial Flyby	4.847	0.030
South Pole Flyby	4.920	0.016
Preliminary Survey Multi-Arc	4.892	0.004
Preliminary Survey Long Arc	4.890	0.006
Orbit A Long Arc	4.8914	0.0003

1.2. Multi-Arc Filtering

For completeness, the derivation of the multi-arc filter used in this work is included. This method is based on the algorithm described in ESA's *NAPEOS (Navigation Package for Earth Observation Satellites) Mathematical Models and Algorithms*,¹⁰ however the algorithm has been re-derived starting from Equation 1.

Partition the Normal Equations:

The standard normal equations for arc i can be arranged such that the local arc parameters, a , and global parameters, g , are partitioned into the form

$$\begin{bmatrix} N_a^i & N_{ag}^i \\ N_{ag}^{iT} & N_g^i \end{bmatrix} \begin{bmatrix} \Delta \mathbf{x}_a^i \\ \Delta \mathbf{x}_g^i \end{bmatrix} = \begin{bmatrix} \mathbf{B}_a^i \\ \mathbf{B}_g^i \end{bmatrix} \quad (1)$$

which expanded is

$$N_a^i \cdot \Delta \mathbf{x}_a^i + N_{ag}^i \cdot \Delta \mathbf{x}_g^i = \mathbf{B}_a^i \quad (2)$$

$$N_{ag}^{iT} \cdot \Delta \mathbf{x}_a^i + N_g^i \cdot \Delta \mathbf{x}_g^i = \mathbf{B}_g^i \quad (3)$$

The sub matrices in the above expression can be extracted directly from a batch least squares filter

$$\begin{aligned} N_a^i &= P_{0a}^{i-1} + H_a^{iT} \cdot W^i \cdot H_a^i \\ N_g^i &= P_{0g}^{i-1} + H_g^{iT} \cdot W^i \cdot H_g^i \\ N_{ag}^i &= H_a^{iT} \cdot W^i \cdot H_g^i \\ \mathbf{B}_a^i &= P_{0a}^{i-1} \cdot \Delta \mathbf{x}_{0a}^i + H_a^{iT} \cdot W^i \cdot \Delta \mathbf{y}^i \\ \mathbf{B}_g^i &= P_{0g}^{i-1} \cdot \Delta \mathbf{x}_{0g}^i + H_g^{iT} \cdot W^i \cdot \Delta \mathbf{y}^i \end{aligned}$$

where P_0 are the *a-priori* covariances, H are the measurement mappings, W are the observation weightings, $\Delta \mathbf{y}$ are the *pre-fit* residuals and $\Delta \mathbf{x}_0$ are the *a-priori* deviations as computed from a converged solution

$$\begin{aligned} \Delta \mathbf{x}_{0a}^i &= \mathbf{x}_a^i - \mathbf{x}_{0a}^i \\ \Delta \mathbf{x}_{0g}^i &= \mathbf{x}_g^i - \mathbf{x}_{0g}^i \end{aligned}$$

Solve for Global Parameters:

Pre-multiply Equation 2 by $(-N_{ag}^{iT} \cdot N_a^{i-1})$ and combine with Equation 3 to eliminate the local terms. This yields

$$(N_g^i - N_{ag}^{iT} \cdot N_a^{i-1} \cdot N_{ag}^i) \cdot \Delta \mathbf{x}_g^i = \mathbf{B}_g^i - N_{ag}^{iT} \cdot N_a^{i-1} \cdot \mathbf{B}_a^i$$

which, for simplicity, can be written more compactly as

$$N_g^{i*} \cdot \Delta \mathbf{x}_g^i = \mathbf{B}_g^{i*} \quad (4)$$

Equation 4 cannot be solved as written because x_g^i is different for each arc. In order to solve for a single best estimate assume that each arc would converge to the same estimate χ_g given one more iteration. Equation 4 can now be rewritten as

$$N_g^{i*} \cdot (\hat{\mathbf{x}}_g - \chi_g + \chi_g - \mathbf{x}_g^i) = \mathbf{B}_g^{i*}$$

Rearranging and summing over each arc yields the common estimate of the global parameters, along with the updated covariance

$$\hat{\mathbf{x}}_g = \chi_g + \left(\sum N_g^{i*} \right)^{-1} \cdot \sum \left(\mathbf{B}_g^{i*} + N_g^{i*} (\mathbf{x}_g^i - \chi_g) \right) \quad (5)$$

$$\hat{P}_g = \left(\sum N_g^{i*} \right)^{-1} \quad (6)$$

a-priori uncertainty, P_χ , about χ_g can be included

$$\hat{\mathbf{x}}_g = \chi_g + \left(P_\chi^{-1} + \sum N_g^{i*} \right)^{-1} \cdot \sum \left(\mathbf{B}_g^{i*} + N_g^{i*} (\mathbf{x}_g^i - \chi_g) \right) \quad (7)$$

$$\hat{P}_g = \left(P_\chi^{-1} + \sum N_g^{i*} \right)^{-1} \quad (8)$$

Note that the selection of suitable χ_g is somewhat arbitrary and P_χ^{-1} , the *a priori* information of χ_g , should nominally be set to zero. It has been found that in most cases the final solution is insensitive to the selection method for χ_g so long as each arc is converged and the state is fully observable.

Solve for Local Parameters:

Substitute the updated global solution back into Equation 1 and expand to get

$$N_a^i \cdot \Delta \mathbf{x}_a^i + N_{ag}^i \cdot \Delta \hat{\mathbf{x}}_g^i = \mathbf{B}_a^i \quad (9)$$

$$N_{ag}^{iT} \cdot \Delta \mathbf{x}_a^i + \hat{N}_g \cdot \Delta \hat{\mathbf{x}}_g^i = \hat{\mathbf{B}}_g \quad (10)$$

where $\hat{N}_g = \hat{P}_g^{-1}$ and $\hat{\mathbf{B}}_g = \sum \left(\mathbf{B}_g^{i*} + N_g^{i*} (\mathbf{x}_g^i - \chi_g) \right)$. Similar to above, pre-multiply 10 by $(-N_{ag}^i \cdot \hat{N}_g^{-1})$ and combine with 9 to isolate the local parameters

$$(N_a^i - N_{ag}^i \cdot \hat{P}_g \cdot N_{ag}^{iT}) \cdot (\hat{\mathbf{x}}_a^i - \mathbf{x}_a^i) = \mathbf{B}_a^i - N_{ag}^i \cdot \hat{P}_g \cdot \hat{\mathbf{B}}_g$$

which results in the multi-arc solution for the local parameters

$$\hat{\mathbf{x}}_a^i = \mathbf{x}_a^i + (N_a^i - N_{ag}^i \cdot \hat{P}_g \cdot N_{ag}^{iT})^{-1} \cdot (\mathbf{B}_a^i - N_{ag}^i \cdot \hat{P}_g \cdot \hat{\mathbf{B}}_g) \quad (11)$$

$$\hat{P}_a^i = (N_a^i - N_{ag}^i \cdot \hat{P}_g \cdot N_{ag}^{iT})^{-1} \quad (12)$$

for each i . The multi-arc post-fit residuals for each arc can then be computed

$$\Delta \hat{\mathbf{y}}^i = \Delta \mathbf{y}^i - H_a^i \cdot (\hat{\mathbf{x}}_a^i - \mathbf{x}_a^i) - H_g^i \cdot (\hat{\mathbf{x}}_g - \mathbf{x}_g^i) \quad (13)$$

References

¹P. G. Antreasian, et al, "Early Navigation Performance from the OSIRIS-REx Approach to Bennu," *AAS Guidance and Control Conference*, Breckenridge, CO, Feb. 2019.

²B. Williams, P. Antreasian, E. Carranza, C. Jackman, J. Leonard, D. Nelson, B. Page, D. Stanbridge, D. Wibben, K. Williams, M. Moreau, K. Berry, K. Getzandanner, A. Liounis, A. Mashiku, D. Highsmith, B. Sutter, and D. S. Lauretta, "OSIRIS-REx Flight Dynamics and Navigation Design," *Space Sci Rev*, June 2018, pp. 1–43.

³J. M. Leonard, et al, "OSIRIS-REx orbit determination performance during the navigation campaign," *AIAA/AAS Astrodynamics Specialist Conference*, Portland, ME, Aug. 2019.

⁴D. J. Scheeres, et al, “The dynamic geophysical environment of (101955) Benu based on OSIRIS-REx measurements,” *Nature Astronomy*, Mar. 2019, pp. 1–10.

⁵W. M. Kaula, *Theory of Satellite Geodesy*. Applications of Satellites to Geodesy, University of California at Los Angeles: Blaisdell Publishing Company, 1966.

⁶J. K. Miller, A. S. Konopliv, P. G. Antreasian, J. J. Bordi, S. Chesley, C. E. Helfrich, W. M. Owen, T. C. Wang, B. G. Williams, D. K. Yeomans, and D. J. Scheeres, “Determination of Shape, Gravity, and Rotational State of Asteroid 433 Eros,” *ICARUS*, Vol. 155, Jan. 2002, pp. 3–17.

⁷A. Genova, L. Iess, and M. Marabucci, “Mercury’s gravity field from the first six months of MESSENGER data,” *Planetary and Space Science*, Vol. 81, June 2013, pp. 55–64.

⁸P. Tortora, M. Zannoni, D. Hemingway, F. Nimmo, R. A. Jacobson, L. Iess, and M. Parisi, “Rhea gravity field and interior modeling from Cassini data analysis,” *ICARUS*, Vol. 264, Jan. 2016, pp. 264–273.

⁹S. R. Chesley, D. Farnocchia, M. C. Nolan, D. Vokrouhlický, P. W. Chodas, A. Milani, F. Spoto, B. Rozitis, L. A. M. Benner, W. F. Bottke, M. W. Busch, J. P. Emery, E. S. Howell, D. S. Lauretta, J.-L. Margot, and P. A. Taylor, “Orbit and bulk density of the OSIRIS-REx target Asteroid (101955) Benu,” *ICARUS*, Vol. 235, June 2014, pp. 5–22.

¹⁰European Space Operation Centre, “NAPEOS - Navigation Package for Earth Orbiting Satellites,” May 2009, pp. 1–150.